Available online at www.sciencedirect.com
ScienceDirect
Polymer 48 (2007) 5486–5492
polymer
www.elsevier.com/locate/polymer

Polymer Communication

Hierarchical crystalline structure of HDPE molded by gas-assisted injection molding

Guo-Qiang Zheng [a,b], Li Huang [a], Wei Yang [a], Bin Yang [a], Ming-Bo Yang [a,*], Qian Li [b], Chang-Yu Shen [b]

[a] College of Polymer Science and Engineering, State Key Laboratory of Polymer Materials Engineering, Sichuan University, Chengdu 610065, China
[b] College of Material Science and Engineering, National Engineering Research Center for Advanced Polymer Processing Technology, Zhengzhou University, Zhengzhou 450002, China

Received 9 November 2006; received in revised form 9 May 2007; accepted 16 May 2007
Available online 25 May 2007

Abstract

To understand the crystalline morphology of the parts molded by gas-assisted injection molding (GAIM), in this work, the hierarchical structures and the crystalline morphology of gas-assisted injection molded high-density polyethylene (HDPE) were investigated. According to the comparison between the results of the GAIM part and those of the conventional injection molded counterpart, it is found that gas penetration can remarkably enhance the shear rate during GAIM process and oriented lamellar structure, shish–kebab structure and common spherulites arise in the skin, subskin and gas channel region, respectively, owing to the different shear rate in these regions. Meanwhile, cooling rate also plays an important role in the formation of the oriented crystalline structure.

Keywords: Gas-assisted injection molding; Gas penetration; Shish–kebab structure

1. Introduction

Gas-assisted injection molding (GAIM), an innovative molding process [1,2], has been developed on the basis of conventional injection molding (CIM). Its main feature is that the mold cavity is partially filled with polymer melt, and then compressed gas penetrates the molten polymer and drives it further into the mold end until the cavity is completely occupied. A schematic representation of this technology is shown in Fig. 1. GAIM has drawn intensive attention for its excellent advantages [3–6], such as significantly reducing material cost, clamping tonnage, cycle time and prolonging the life-span of injection machine. In addition, some defects encountered in CIM, such as residual stress, warpage, sink marks can be substantially eliminated, especially for the large parts whose quality and rigidity are the main concerns.

It is well known that polymer melt is subjected to a complex thermo-mechanical field characterized by rapid cooling rate and severe stress field during CIM process, and these fields vary along the flow path and through the thickness of the parts. As a result, a CIM part usually shows an intrinsic heterogeneous microstructure, featuring a gradual and hierarchical variation of the morphology that evolves throughout the part. Many studies [7–9] showed that neat crystalline polymers molded by CIM are always characterized with multilayered structure in accordance with the crystalline morphology and size, that is, a highly oriented nonspherulitic skin, a row or shear-nucleated spherulitic subskin, and a typically spherulitic core.

It should be noted that, during CIM process, the melt is merely confined by the mold wall, i.e. a rigid and cold medium. However, during the gas penetration of the GAIM process, the melt is confined not only by the mold wall but also by the compressed gas. Whether the different confining media with widely different physical properties would lead to distinct different flow behaviors, and then the flow behaviors give rise

* Corresponding author.
E-mail address: yangmb@scu.edu.cn (M.-B. Yang).

0032-3861/$ - see front matter © 2007 Published by Elsevier Ltd.
doi:10.1016/j.polymer.2007.05.047

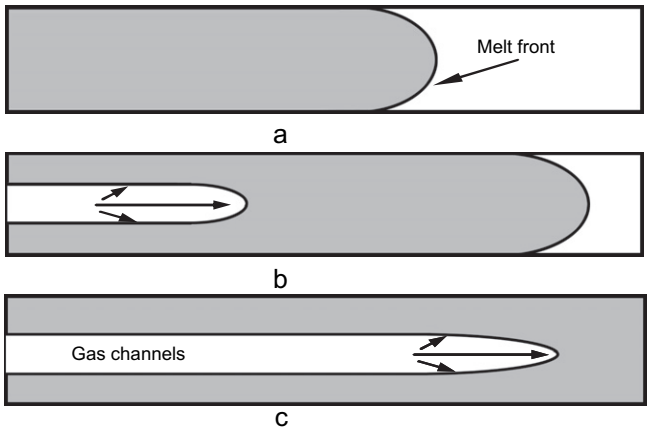

Fig. 1. Schematic representation of GAIM: (a) short shot; (b) gas penetration; (c) gas-assisted packing.

to different microstructures? Recently, we reported the unusual phase morphology of PC/PE blend molded by GAIM, in which the stronger shear field brought by gas penetration is responsible for such a phenomenon [10], which has substantiated our hypothesis. Now that the unusual phase morphology can be formed during GAIM process, could fascinating crystalline morphology come into being? Unfortunately, little work has been done in this field.

In this communication, our interest is in the crystalline morphology of neat HDPE molded by GAIM. For comparison, the crystalline morphology of that molded by CIM was also investigated. From a practical point of view, attempting to explore the crystallization characteristics during the GAIM process which has been widely used in practical production is of great significance.

2. Experimental part

2.1. Material

The resin used in this study is HDPE (5000S). It was a commercial product of DaQing Petroleum Chemical Co., China, supplied in pellets with number-average molecular weight of 5.28×10^5 g/mol. Its melt flow rate is 0.9 g/10 min (21.6 N, 190 °C).

2.2. Sample preparation

Using the same mold depicted in literature [10], two kinds of columnar parts of the same shape were molded, respectively, by GAIM and CIM. In order to provide a routeway for gas penetration, the main body of the parts is designed in a columned shape. The main body of the CIM part exhibits a solid structure, while that of the GAIM part takes on a hollowed one.

A Grand 140-320 injection molding machine and a gas injection system (model MPC) with five-stage pressure profile control were employed for the molding process. During GAIM process, only one stage of gas injection was used in this work. Two kinds of GAIM parts were prepared with different gas pressures, i.e., 16.5 and 19.3 MPa. For the sake of brevity, according to the applied gas pressure, the GAIM parts molded with 16.5 and 19.3 MPa are denoted as G16 and G19, respectively. Other processing parameters for GAIM process are listed in Table 1. During the molding process, the temperature profile of the injection molding machine was 120, 150, 170, 185 and 180 °C from hopper to nozzle. The mold temperature was about 30 °C. GAIM and CIM processes were of the same processing condition, except that the melt in CIM process was not exposed to gas penetration and gas-assisted packing process. It should be noted that the melt injection volume for CIM is as large as 100 vol.%.

2.3. Characterization

The 2D wide-angle X-ray scattering experiments were conducted using a SEIFERT diffractometer (DX-Mo8*0.4-S, 40 kV). The wavelength of the monochromated X-ray from Mo radiation was 7.1073×10^{-2} nm and transmission mode was used. The samples were placed with their orientation (flow direction) perpendicular to the beams.

Thermal analysis was performed with a heating rate of 10 °C/min using a Netzsch DSC 204 differential scanning calorimeter.

Selective etching was employed as an appropriate technique to prepare the specimens for SEM observation of the crystalline morphology. Before etching, the GAIM and CIM parts were cut into a 5 mm length segment in the middle of the bar and then cryogenically fractured in liquid nitrogen by sudden bending of the samples along the flow direction. Subsequently, specimens were etched according to the permanganic etching technique developed by Olley and colleagues [11–14]. After the surface was coated with gold powder, the crystalline morphology in different regions of these parts was observed using a SEM instrument, JSM-5900LV, operating at 20 kV.

It should be noted that the samples for 2D-WAXS, DSC and SEM tests were taken from the same regions parallel to the flow direction.

3. Results and discussion

Fig. 2a and b shows the 2D-WAXS patterns in different zones of G16 and CIM part. For G16 (Fig. 2a), one observes obvious reflections of (110) plane of the skin and subskin in equatorial direction, which indicates that there is obvious

Table 1
Processing conditions for GAIM

Parameters	Values
Injection pressure (MPa)	80
Delay time (s)	1
Gas packing time (s)	15
Cool time (s)	60
Short shot size (vol.%)	85

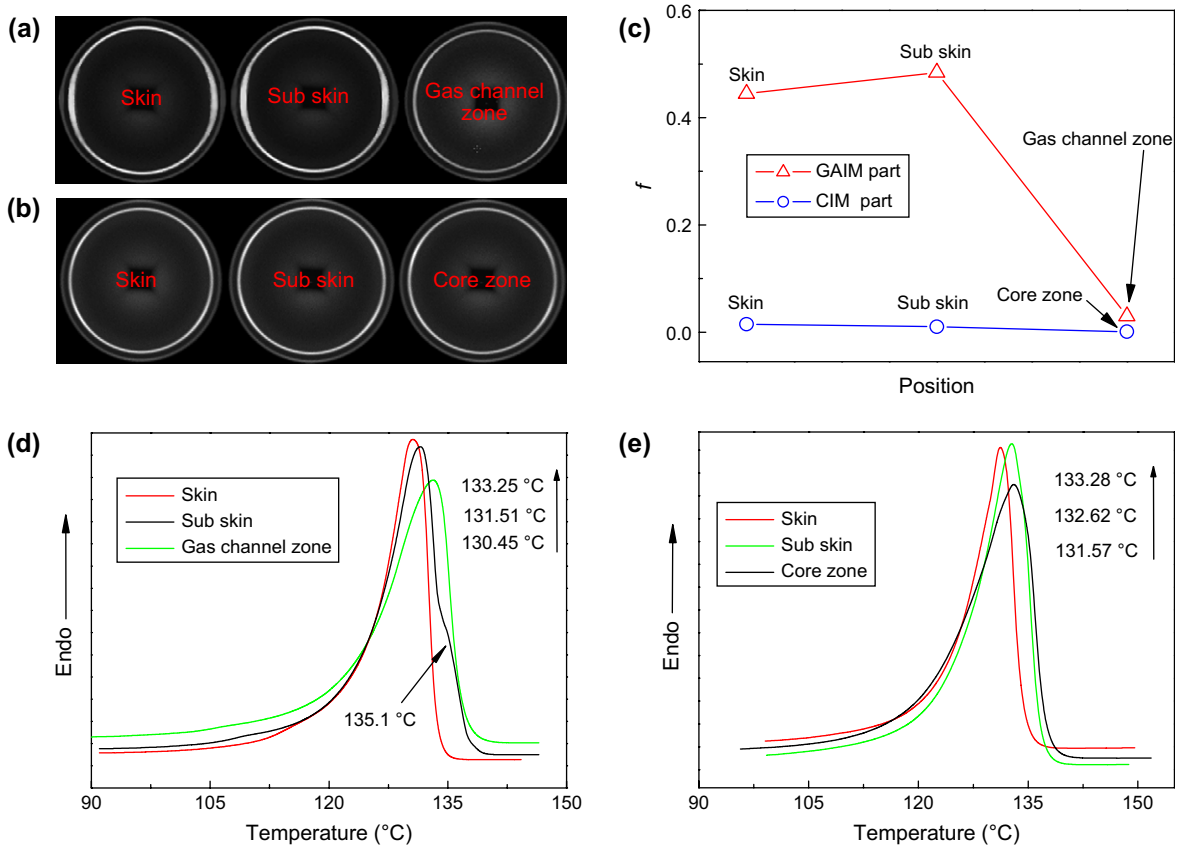

Fig. 2. 2D-WAXS patterns (a, b) and corresponding orientation parameters (c) as well as the DSC results (d, e); (a) and (d) are the samples from G16; (b) and (e) are the samples from the CIM part.

orientation along the flow direction (i.e. vertical direction). In the gas channel zone, one observes two circles rather than arcs, indicating a random orientation. The orientation for G19 layer was also characterized via 2D-WAXS which appeared to follow the same trend as that of G16. For the CIM part (Fig. 2b), two circles rather than arcs are observed in each zone, i.e. preferred orientation does not exist.

The orientation parameter can be quantitatively calculated using the Hermans orientation parameter described in literature [15]. The orientation parameters in different zones of G16 and CIM part are shown in Fig. 2c. For G16, the typical skin-core structure in the direction of thickness is very obvious. The orientation parameter at the subskin is slightly larger than that at the skin. Unexpectedly, it is about zero in the gas channel zone. For the CIM part, orientation parameters are about zero in the three zones, implying that chains align randomly.

Fig. 2d and e, respectively, shows the DSC heating curves at different regions of G16 and the CIM part. For G16, only one main melting peak, around 131 °C, is observed in the skin and gas channel zone. Interestingly, there is a shoulder melting peak, around 135 °C, in the subskin, which indicates that there might be another crystalline structure (most likely shish–kebab structure) existing. For the CIM part, only a melting peak is observed in each zone. These melting peaks, which are around 132 °C, might be attributed to the lamellar melting of spherulites. For both G16 (Fig. 2d) and the CIM part (Fig. 2e), it should be noted that the melting temperature of each zone increases steadily away from the skin toward the inner zone. In addition, from the skin to the inner zone, the melting temperature of each zone in the CIM part is generally higher than that of the corresponding one in G16.

Fig. 3a–c shows the SEM micrographs, in the skin, the subskin and the gas channel zone, respectively, of G16. As shown in Fig. 3a, the fine and parallel lamella stacks, perpendicular to the melt flow direction, dominate the skin. The thickness of the lamella is about 7 nm and the thickness of such morphology evolution is about 150 μm along the residual thickness direction. However, there is no direct evidence of the presence of the extended chain structures (shish) in this region. Due to its rotational component, shear flow is often considered to be a ‘weak’ flow, unable to provide extension of polymer chains or induce shish formation [16]. However, fascinating crystalline morphology like centipede appears in the subskin (Fig. 3b). One can easily identify shish and overgrown lamellar structures which are parallel and perpendicular to the flow direction. Such a structure is well in line with the features of the so-called shish–kebab structure described in literatures [17–19]. It can also be seen that the shish structure is not a continuous homogeneous entity, and its length is in a range of distribution, which could be as small as 3 μm, and as large as 7 μm. Unfortunately, the alignment of molecular chains in

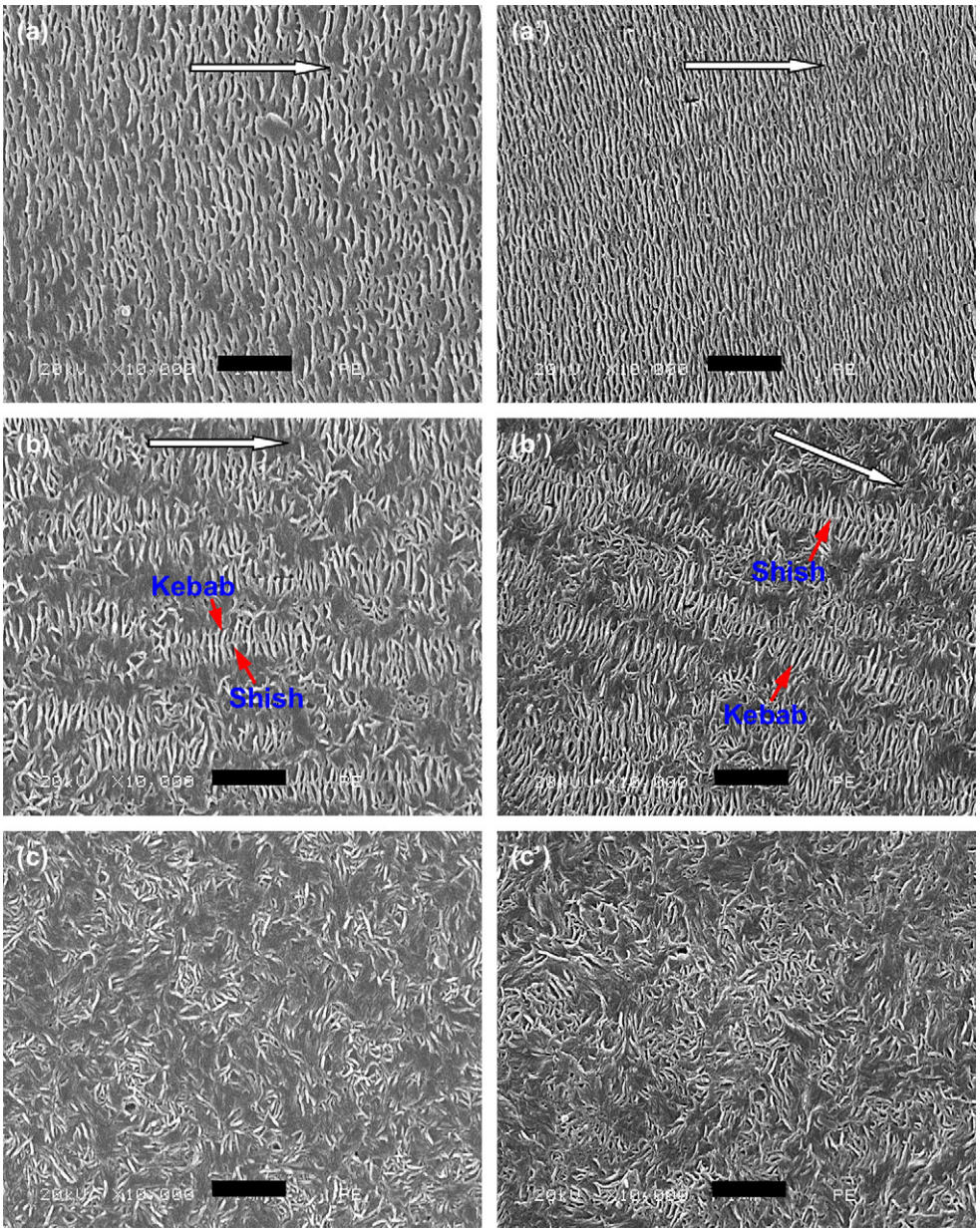

Fig. 3. SEM microphotographs of GAIM samples at a magnification of 10,000; (a–c) are from G16 and (a′–c′) are from G19; a and a′: skin; b and b′: subskin; c and c′: gas channel zone; the arrows represent flow direction.

the shish is out of the resolution of SEM so that, here, it is not discussed in detail. Yet, it is worth to be further investigated. The width of the shish–kebab structure is generally invariable, which is about 1 μm. To the best of our knowledge, however, it is for the first time that such an interesting morphology formed in GAIM part is reported. The shish–kebab structure could be frequently found in the special stress field involved in the instruments for experiments, such as dynamic packing injection molding (oscillating injection molding) [20–22] and vibration-assisted injection molding [23]. Yet, they are scarcely obtained via the common polymer processing methods [24]. Despite the shish–kebab structure could be formed upon gas penetration, it is less denser, compact and highly aligned than that formed through dynamic packing injection molding [25,26]. In the gas channel zone (Fig. 3c), the lamellae primarily show a random arrangement without any evidence of orientation. One observes that the lamellae coalesce into a few ''snowballs'' whose diameter is about 2 μm. Therefore, the gas channel zone is principally characterized with spherulites.

Fig. 3a′–c′ shows the SEM micrographs of etched surface of G19. It is clear that the trend of morphological evolution, from the skin to the gas channel zone, is similar to that of G16. In a word, the two parts molded with different gas pressures are of the similar hierarchical crystalline structure macroscopically. However, there is a slight difference in size between the structures in the corresponding regions of the G16 and G19, e.g. the parallel lamellar stacks of G19 (Fig. 3a′) are more compact than that of G16 (Fig. 3a), and

the shish–kebab structure in G19 (Fig. 3b′) is obviously longer than that of G16 (Fig. 3b). Such a case indicates that gas pressure could influence the crystalline size and aligning degree. In view of this, our future work would be to deal with the influence of processing parameters on the crystalline structure formed by GAIM. The finely aligned lamellae and shish–kebab structure formed in the GAIM process substantiate that GAIM process can also provide the prerequisite stress field for such structure formation. Hence, how the microstructure evolves in GAIM process might become an interesting domain.

Fig. 4 shows the SEM micrographs of etched surface of the CIM part. The lamellae exhibit random distribution not only in the skin (Fig. 4a) but also in the core zone (Fig. 4b), and they always associate into ‘‘snowballs’’. The main crystalline feature in the subskin is also of such morphology, which is omitted here. The ‘‘snowball’’ is the so-called spherulite, whose diameter is as large as 3 μm in the skin and 4 μm in the core zone. Apparently, the common spherulites are predominant not only in the skin but also in the core zone, that is, on the whole etched surface. In summary, the hierarchical crystalline structure is not distinct for the CIM part. Additionally, the size of the spherulite is steadily larger than that of the GAIM part.

It is well known that CIM process is essentially a flow-induced nonisothermal crystallization process for semicrystaline polymer. The shear gradient from the skin to the core zone favourably leads to different degree of crystalline orientation and chain stretching in different regions. The crystalline morphology is determined by shear rate, shear stress and cooling rate and so on. For example, when shear rate exceeds a critical value [27,28], the shear-induced coil-to-stretch transition of polymer chains can result in the preferred orientation structure, namely, the shish–kebab structure [22,29–32]. Here, the cavity of the mold used has a relative large diameter, namely, 10 mm. As a result, the shear rate gradient from the skin to the core layer is relatively inconspicuous when molten plastic is injected into the cavity at a given injection pressure. As the shear rate is relatively small, it could not reach the critical value for the orientation structure (such as the parallel lamella stacks and shish–kebab) formation. Thus, it is understandable that there is no preferred orientation structures found in the CIM part. Additionally, it is well-established that the orientation of polymer chains results from the competition between shear-induced orientation, chain stretching and subsequent relaxation [33]. That is, a larger shear rate leads to a higher orientation of molecular chains, while a faster cooling rate slows down the relaxation and even freezes the orientation by the kick-in of crystallization [15]. During melt filling, once the melt contacts with the cold mold wall, it is reasonable that the stretched and oriented molecules are always prone to be frozen suddenly. However, because of the larger diameter of the mold cavity, at the end of the filling during CIM process, the bulk heat is tremendous. In return, heat in the core is transferred slowly to the skin. While the heat in the core of the mold cavity transfers to the skin, obviously, the cooling rate in the skin should be slowed down. Owing to the above reasons, even though preferred crystalline structures (parallel lamellae and shish–kebab structures) can be formed, which is induced by melt filling, they might relax subsequently during cooling. Thus, preferred crystalline structure is not observed in the CIM part.

To understand the preferred crystalline structure formation mechanisms during the GAIM process, the flow behaviors in the separated filling stages (such as short shot and gas penetration process) should be made clear. As mentioned above, more processing parameters are introduced to GAIM process, thereby the flow behavior during this process is much more complicated than that in CIM process. During the short shot stage, the melt is injected into the cavity under the same conditions as those in the filling stage of the CIM process, with the exception that the melt volume filled in short shot stage is smaller than that in the latter. Hence, not only in the short shot but also in the CIM process, the molecules are almost exposed to the same shear field. In return, the deformation and orientation in the two processes are of the same mechanisms. Recalling the common spherulites in the CIM part, it is evident that the preferred crystalline structure of the GAIM part is formed in the gas penetration stage and the subsequent cooling stage.

Generally, the gas used in GAIM process is regarded as ‘‘inert gas’’, and there is no chemical reaction with melt. As

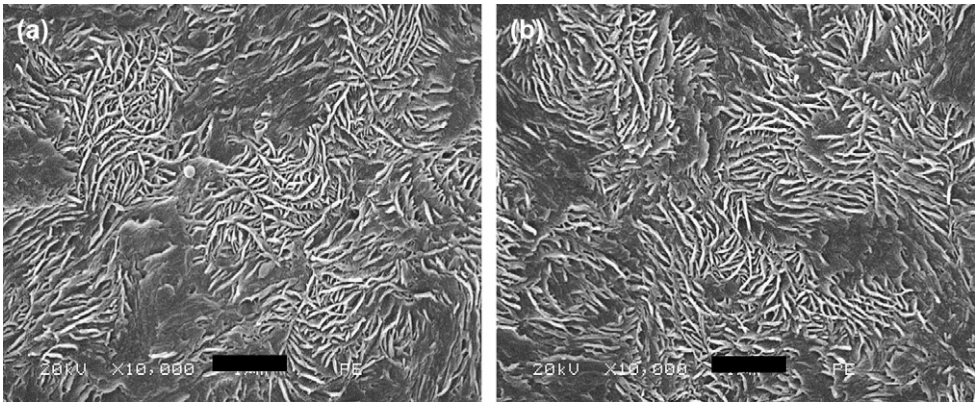

Fig. 4. SEM microphotographs of CIM part at a magnification of 10,000; (a) skin; (b) core zone.

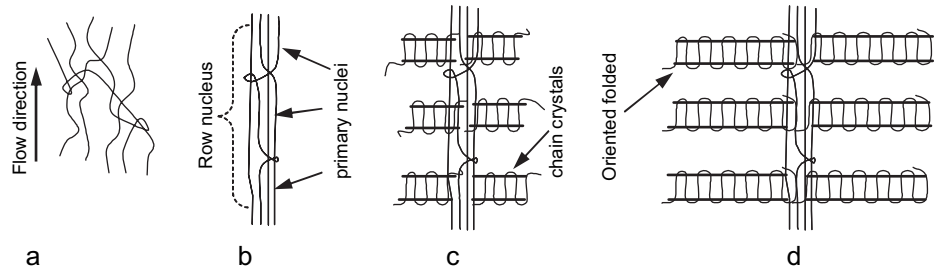

Fig. 5. Schematics of the shear-induced row nuclei and subsequent growth of oriented folded chained crystals. (a) The slight orientation and entanglement of chains at the end of delay time; (b) formation of row nucleus in the flow direction; (c) oriented folded chain lamellae (kebabs) grow from the primary nuclei; (d) the resultant shish–kebab structure.

a result, during the gas penetration process, the compressed gas merely propels the melt around the gas front, but not the one adjacent to the gas channel forwards. In return, there scarcely exists orientated structure in the gas channel zone, and Fig. 3c and Fig. 3c′ firmly corroborate our conjecture. As mentioned in our previous study [10], the nitrogen gas is of much smaller viscous coefficient and larger diffusibility [34], especially under supercritical condition [35] during the gas penetration. Such a gas is much more efficient in transmitting the pressure needed to propel the melt amid the mold cavity to fill the whole cavity. Therefore, the shear rate induced by gas penetration in GAIM process is significantly larger than that in the filling of CIM process. In addition, as reported in our previous studies [10,36], during GAIM process, the shear rate in the subskin is unexpectedly larger than that in the skin, which is different from that in CIM process [7–9]. In contrast to the common shear rate gradient in CIM process, the unusual gradient brought about by gas penetration, after the short shot, plays a significant role in promoting the shear rate, which is deviated from the polymer/mold wall interface. In a word, the resultant morphology in different regions of the GAIM parts must be primarily related to gas penetration.

It is well believed that, upon application of the shear, the polymer chains in the melt extend in the direction of shear field and form extended microfibrillar structures. However, at a given molecular weight and temperature field, the degree of orientation from the initial random coil conformation and the extent of their alignment will, obviously, vary depending on the external conditions [37]. For the GAIM process, owing to the shear rate in the skin which might not reach the critical value for shish–kebab formation, only some of the chain segments of the molecule are aligned in the flow direction, and the other segments, especially those near the chain ends, remain in random distribution. In such a case, a tiny cluster of oriented chain segments could be formed in the skin, and this cluster may further act as a primary nucleus. Subsequently, oriented folded chain lamellae (kebabs) grow radially outward in the perpendicular direction to the microfibril (cluster of oriented chain segments) axis. Such a growth process of the oriented lamellae is similar to that depicted in detail in literature [37]. In the subskin, the stronger shear rate which might exceed the critical value for shish–kebab formation, may induce more and longer chain segments to orient, and develop into more clusters of oriented chain segments, or even much longer fibrils of stretched chains. Such clusters or fibrils of the oriented chain segments can be lined in the shear rate direction, namely the row nuclei in the form of microfibrillar bundles, with many primary nuclei on them. These primary nuclei promote the epitaxial growth of folded chain lamellae that filled the space normal to the row nuclei until they impinged on each other. And thus, the shish–kebab structure is formed. In view of the relatively small shear rate in short shot process, the possible chain relaxation during delay time as well as the extremely short time for gas penetration, it is impossible for the chains in the subskin to adjust themselves to a fully extended state, i.e. certain sections of a chain can be fully extended while remaining sections lose orientation or even entangles with others [38,39]. For these reasons, a modified shish–kebab growth model can be illustrated by Fig. 5. Fig. 5a illustrates the slight orientation and entanglement of chains in the melt at the end of delay time in GAIM process. Fig. 5b shows the formation of a row nucleus in the flow direction, which comprises a few primary nuclei. Fig. 5c represents that oriented folded chain lamellae (kebabs) grow, from the primary nuclei, radially outward and normal to the row nuclei. Fig. 5d depicts the final shish–kebab structure, which includes the stacks of lamellae perpendicular to the flow direction. Thanks to the relative low shear rate, it is understandable that the crystalline feature in the core layer is spherulites.

Furthermore, the cooling rate also plays an effective role in the preferred crystalline structure formation. At the end of gas penetration in GAIM process, the core region of the mold cavity is hollowed out by gas. Thereby the residual wall of the GAIM part is formed and the residual thickness of the wall becomes notably thin (here, the residual thickness is about 1.7 mm). Owing to the thinner residual wall of the GAIM part, a pronounced heat exchange between the mold wall and the part occurs. Then, the orientation structure induced by shear rate could be cooled down rapidly and reserved subsequently.

4. Conclusions

Apart from the common spherulites, parallel lamella stacks and fascinating shish–kebab structure are formed in the GAIM part. The fierce shear rate brought about by the gas

penetration and the fast cooling rate are two principal factors in such a structure formation. Since the shish–kebab structure may greatly improve mechanical properties, naturally, it will be our future work to study the further mechanism of such preferred crystalline morphology formation and the relationship between such structures and their mechanical properties.

Acknowledgements

The authors gratefully acknowledge the financial support of this work by the National Nature Science Found of China (Grant nos. 10590351, 50673067 and 10372095) and the Major State Basic Research Projects (Grant no. 2005CB623808).

References

[1] Stevens Tim. Mater Eng 1991;108:28–9.
[2] Turng LS. Adv Polym Technol 1995;14:1–13.
[3] Li CT. Polym Eng Sci 2004;44:992–1004.
[4] Chen SC, Hsu KS, Hung JS. Ind Eng Chem Res 1995;34:416–20.
[5] Turng LS. Adv Polym Technol 1997;16:159–73.
[6] Chien RD, Chen SC, Chen YC. Plast Rubber Compos 2002;31:336–43.
[7] Daly HB, Sanschagrin B, Nguyen KT, Cole KC. Polym Eng Sci 1999;39:1736–51.
[8] Victor T, Kamal MR. J Appl Polym Sci 1978;22:2341–52.
[9] Knatz MR, Newman HD, Stigale FH. J Appl Polym Sci 1972;16:249–57.
[10] Zheng GQ, Yang W, Yin B, Yang MB, Liu CT, Shen CY. J Appl Polym Sci 2006;102:3069–77.
[11] Friedrich K, Ueda E, Kamo H, Evstatiev M, Krasteva B, Fakirov KI. J Mater Sci 2002;37:4299–305.
[12] Olley RH, Bassett DC. Polymer 1982;23:1707–10.
[13] Bassett DC, Olley RH. Polymer 1984;25:935–43.
[14] Freedman AM, Bassett DC, Vaughan AS, Olley RH. Polymer 1986;27:1163–9.
[15] Zhong GJ, Li LB, Mendes M, Byelov D, Fu Q, Li ZM. Macromolecules 2006;39:6771–5.
[16] Keller A, Kolnaar HWH. In: Meijer HEH, editor. Processing of polymers, vol. 18. New York: VCH; 1997. p. 189.
[17] Hosier IL, Bassett DC. Polymer 1995;36:4197–202.
[18] Daniel D, Marom G, Avila-Orta CA, Somani RH, Hsiao BS. Polymer 2005;46:3096–104.
[19] Zhang CG, Hu HQ, Wang DJ, Yan SK, Han CC. Polymer 2005;46:8157–61.
[20] Kalay G, Sousa RA, Reis RL, Cunha AM, Bevis MJ. J Appl Polym Sci 1999;73:2473–83.
[21] Guan Q, Lai FS, McCarthy SP, Chiu D, Zhu XG, Shen KZ. Polymer 1997;38:5251–3.
[22] Wang Y, Na B, Fu Q, Men YF. Polymer 2004;45:207–15.
[23] Li YB, Liao YH, Gao XQ, Yuan Y, Ke WT, Shen KZ. J Polym Sci Part B Polym Phys 2005;43:13–5.
[24] Martinez-Salazar J, Garcia Ramos JV, Petermann J. Int J Polym Mater 1993;21:111–21.
[25] Cao W, Wang K, Zhang Q, Du RN, Fu Q. Polymer 2006;47:6857–67.
[26] Liang S, Wang K, Yang H, Zhang Q, Du RN, Fu Q. Polymer 2006;47:7115–22.
[27] Dukovski I, Muthukumar M. J Chem Phys 2003;118:6648–55.
[28] Li L, de Jeu WH. Phys Rev Lett 2004;92:1–3.
[29] Katti SS, Schultz JM. Polym Eng Sci 1982;22:1001–17.
[30] Lotz B, Wittmann JC, Lovinger AJ. Polymer 1996;37:4979–92.
[31] Monks AW, White HM, Bassett DC. Polymer 1985;26:5933–6.
[32] Kumaraswamy Guruswamy, Verma Ravi K, Kornfield Julia A, Yeh Fengji, Hsiao Benjamin S. Macromolecules 2004;37:9005–17.
[33] Doi M, Edwards SF. The theory of polymer dynamics. Oxford, UK: Clarendon; 1986.
[34] Reid RC, Prausnitz JM, Poling BE. The properties of gases and liquids. 4th ed. New York: McGraw Hill; 1987. p. 738.
[35] Wang DY, Wang J, Qu XZ, Liang RF, Qi ZN. Acta Polym Sin 2000;44:111–4.
[36] Zheng GQ, Yang W, Huang L, Yang MB, Li W, Liu CT, et al. Mater Lett 2007;61:3436–9.
[37] Somani Rajesh H, Hsiao Benjamin S, Nogales Aurora. Macromolecules 2000;33:9385–94.
[38] Hsiao BS, Yang L, Somani RH, Avila-Orta CA, Zhu L. Phys Rev Lett 2005;94:117802.
[39] Somani RH, Yang L, Zhu L, Hsiao BS. Polymer 2005;46:8587–623.